Sensitivity of the Global Water Cycle to the Water-Holding Capacity of Land

P. C. D. MILLY AND K. A. DUNNE

U.S. Geological Survey, Geophysical Fluid Dynamics Laboratory/NOAA, Princeton, New Jersey

(Manuscript received 16 June 1993, in final form 30 August 1993)

ABSTRACT

The sensitivity of the global water cycle to the water-holding capacity of the plant-root zone of continental soils is estimated by simulations using a mathematical model of the general circulation of the atmosphere, with prescribed ocean surface temperatures and prescribed cloud. With an increase of the globally constant storage capacity, evaporation from the continents rises and runoff falls, because a high storage capacity enhances the ability of the soil to store water from periods of excess for later evaporation during periods of shortage. In addition to this direct effect, atmospheric feedbacks associated with the resulting higher precipitation and lower potential evaporation drive further changes in evaporation and runoff. Most of the changes in evaporation and runoff occur in the tropics and in the northern middle-latitude rain belts. Global evaporation from land increases by about 7 cm for each doubling of storage capacity in the range from less than 1 cm to almost 60 cm. Sensitivity is negligible for capacity above 60 cm.

In the tropics and in the extratropics, the increased continental evaporation is split, in approximately equal parts, between increased continental precipitation and decreased convergence of atmospheric water vapor from ocean to land. In the tropics, this partitioning is strongly affected by induced circulation changes, which are themselves forced by changes in latent heating. The increased availability of water at the continental surfaces leads to an intensification of the Hadley circulation and a weakening of the monsoonal circulations. In the northern middle and high latitudes, the increased continental evaporation moistens the atmosphere. This change in humidity of the atmosphere is greater above the continents than above the oceans, and the resulting reduction in the sea–land humidity gradient causes a decreased onshore transport of water vapor by transient eddies.

Results established here may have implications for certain problems in global hydrology and climate dynamics, including the effects of water resource development on global precipitation, climatic control of plant rooting characteristics, climatic effects of tropical deforestation, and climate-model errors induced by errors in land-surface hydrologic parameterizations.

1. Introduction

Continental surfaces are an important part of the climate system, because they exchange water and energy with the atmosphere. An important feature of continental surfaces is their ability to absorb and store large amounts of precipitation and later to release the water, as vapor, to the atmosphere. The thin veneer of porous soil and the canopy of vegetation rooted therein are the conduits for intake and release and the vessels for storage. In simplest terms, the soil–vegetation system behaves like a water reservoir whose contents vary in response to fluctuating supplies and demands. The critical parameter is the effective water-holding capacity of the soil. If the capacity is large, precipitation may be stored and later released freely for evaporation. If it is small, much runoff may occur and the soil may dry out often and be unable to supply water for evaporation.

A basic unknown in climate–hydrology interactions is the sensitivity of the global water cycle to the water-holding capacity of land. A world whose continents were solid rock, or whose soil supported no rooted vegetation, might have much smaller effective water-holding capacities than does the earth today, and there might be little evaporation from land. How would the water cycle and climate of such an earth differ from the current one? At the other extreme, one may conceive of an earth where the effective storage capacity is everywhere great enough to maximize evaporation from land; such capacity could come about naturally through greater root development in deeper soils, for example, or through continued development of water storage reservoirs and irrigation by humans. How would the water cycle and climate of such an earth differ from the present situation? And where is the earth of today on the scale between these extremes?

The questions posed above may not have any direct practical significance because of the extreme situations considered. Nevertheless, the closely related question of sensitivities of the water cycle to smaller perturbations in storage capacity is relevant in the fields of global hydrology and mathematical modeling of climate. Many contemporary land-surface changes generate essentially the same hydrologic effects as changes of wa-

Corresponding author address: Dr. P. C. D. Milly, U.S. Geological Survey GFDL/NOAA, P.O. Box 308, Princeton, NJ 08542.

ter-holding capacity, and the associated impacts on surface water balance and climate are directly proportional to the aforementioned sensitivities. Additionally, many of the errors in surface hydrologic parameterizations for climate models may be ascribed to, or otherwise characterized as, errors in the value of an effective storage capacity. It follows that the associated errors in calculated water cycles and climates are directly proportional to these sensitivities.

The general sensitivity problem identified above has two main parts—the sensitivity of surface water and energy balances to the water-holding capacity for a given climate, and the atmospheric sensitivity to the surface water and energy balances. Obviously, feedbacks couple these two parts of the problem. A change in the capacity causes changes in the energy and water fluxes into the atmosphere, resulting in changes of the precipitation, the near-surface atmospheric states, and the radiation fluxes that affect the surface water and energy balances.

The storage capacity of land is at the crux of the hydrology–climate linkage, but little research has been devoted to understanding the role it plays. Some recent studies (Dickinson and Henderson-Sellers 1988; Lean and Warrilow 1989; Shukla et al. 1990; Nobre et al. 1991) of tropical deforestation have, in effect, included changes in land water-holding capacity, but the influence of those changes was masked by the influences of the accompanying prescribed changes in albedo and roughness. The local sensitivity of surface water balance to water-holding capacity, with prescribed atmospheric forcing, (that is, the first half of the sensitivity problem identified above) was investigated by Zubenok (1978), with the finding that a given percentage change of storage capacity typically gives a percentage change in evaporation that is an order of magnitude smaller. Other studies have addressed the atmospheric sensitivity to evaporation (that is, the second half of the sensitivity problem). Shukla and Mintz (1982) compared the climates associated with globally dry and saturated soils, without a requirement for water mass balance of land. They showed that evaporation from land strongly affects climate, especially continental precipitation and temperature. They noted increased rising motion over the continents in the dry soil case, but reported that this did not enhance the precipitation, due to the lack of a continental moisture supply. Yeh et al. (1984) analyzed the transient response of the global hydrologic cycle to an instantaneous, large-scale irrigation. They concluded that additional evaporation tended to enhance precipitation in the model rain belts, regardless of where the evaporation anomaly occurred, and that the tropical irrigation weakened the upward branch of the Hadley circulation in the vicinity of the tropical rain belt. In summary, review of the literature indicates that some pieces of this sensitivity problem have been treated, mostly in a cursory fashion, and that the physical mechanisms, including surface–atmosphere feedbacks, controlling the sensitivities have not been elucidated.

This study has the following objectives: 1) to quantify the sensitivities of the global water cycle in a climate model to the value of the water-holding capacity of the continental surfaces; and 2) to identify the mechanisms and the feedbacks that determine those sensitivities. Section 2 describes the experiment design, which included simulations with interactive continental hydrology and a variety of values for a globally constant water-holding capacity, and simulations in which soils are prescribed to be either wet or dry globally. These were supplemented by stand-alone land-surface simulations, which helped separate the atmospheric feedbacks from the direct effects in the climate experiments. Section 3 is a brief overview of the results of climatic simulations using globally constant water-holding capacities of 4 cm and 60 cm. The results of these two simulations are employed in comprehensive analyses of the continental response (section 4) and of the atmospheric response (section 5) to a change of water-holding capacity. Section 6 generalizes the results of the earlier sections by briefly comparing the results of all simulations. Section 7 contains a summary and discusses implications and limitations of the study.

2. Plan of numerical experiments

a. Description of the model

The numerical experiments were conducted using a general circulation model of the atmosphere, coupled to simple parameterizations of water and energy at the continental surfaces, with prescribed ocean-surface temperatures and cloud distributions. Use of a noninteractive ocean was motivated by computational constraints and by the focus of the study on land–atmosphere interaction. Clouds were prescribed because there is much uncertainty about how clouds should be parameterized in climate models. The neglect of oceanic and cloud radiative feedbacks is an important aspect of this study. Their possible effects are discussed briefly at the end of the paper.

The dynamical component of the general circulation model (Gordon and Stern 1982) approximately solves the three-dimensional, time-dependent transport equations for vorticity, divergence, temperature, and water vapor mixing ratio. The numerical approximations are generated by forming finite differences in time and in the vertical σ coordinate (pressure divided by surface pressure), and by representing horizontal variability by means of a sum (R-15 truncation) of spherical harmonics. The time step is 30 min, and the nine levels of σ are 0.025, 0.095, 0.205, 0.35, 0.515, 0.68, 0.83, 0.94, and 0.99. Nonlinear dynamic terms and surface interactions are computed on a grid with spacings of 7.5° longitude and (on average) 4.5° latitude.

Radiative transfer calculations include the effects of clouds and water vapor. The cloud distribution is pre-

TABLE 1. Summary of climate simulations.

Simulation name	Water-holding capacity (cm)	Soil water (cm)	Spinup duration (yr)	Equilibrium duration (yr)
W1	1	predicted	2	5
W4	4	predicted	2	10
W15	15	predicted	2	5
W30	30	predicted	4	5
W60	60	predicted	8	10
W120	120	predicted	16	5
W240	240	predicted	32	5
DRY	15	0	2	5
SAT	15	15	2	5

scribed, as is the distribution of the snow-free surface albedo. Surface albedo is adjusted interactively for snow cover. The seasonal cycle of solar forcing at the top of the atmosphere is included, but the diurnal cycle is not.

Precipitation occurs when necessary to avoid supersaturation of the atmosphere with respect to water vapor. This may occur as a result of large-scale atmospheric motions or convection. Moist convection is performed by the method of Manabe et al. (1965).

In the simulations with interactive continental hydrology, the land-surface parameterization uses, without modification, Manabe's (1969) implementation of Budyko's (1956) land-surface water- and energy-balance model. A water storage variable, representing the total depth of available water stored in the soil, is calculated at each time step by an accounting of liquid precipitation, snowmelt, evaporation, and runoff. The water-holding capacity of the soil is assumed globally constant. Runoff occurs when saturation of this capacity prevents storage of more water. Evaporation is the product of a potential evaporation rate and a simple function of the ratio of storage to capacity; the potential rate is found by assuming that the air at the surface is saturated at the surface temperature. Land-surface temperature is determined by balancing radiation, sensible heat flux, and latent heat flux. When snow cover is present, sufficient snowmelt is generated to prevent the surface temperature from exceeding the freezing point of water. Surface-layer fluxes are parameterized using a bulk transfer coefficient of 0.003 over land and 0.001 over oceans. For the prescribed-storage simulations, the surface parameterization is essentially the same, but the term identified as runoff is adjusted at the end of each time step (even if negative values are required) to maintain the water storage at the prescribed value (zero or capacity).

The potential evaporation rate calculated using actual surface temperature, $E_p(T_s)$, can differ greatly, when the soil is dry, from that calculated using the hypothetical wet-surface temperature, $E_p(T_w)$ (Milly 1992). Manabe (1969) used the former; Budyko (1956) specified the latter. Milly (1992) showed that the distinction between $E_p(T_s)$ and $E_p(T_w)$ would be important for calculations of potential evaporation and soil moisture in a climate model, but that the actual surface fluxes and climate should be relatively insensitive to the choice of potential evaporation; subsequent sensitivity analyses using the climate model have supported this conclusion. In view of this, and for consistency with many past studies using the same climate model, Manabe's (1969) formulation for evaporation is not modified for the simulations in this study.

Although $E_p(T_s)$ is used to parameterize evaporation in the simulations, the results are analyzed using $E_p(T_w)$ as a more meaningful measure of potential evaporation. This might appear to be inconsistent, but is justified (indeed, motivated) by two considerations. For clarity of analysis, it is desirable that the potential evaporation rate should represent the energy-limited evaporation rate; only $E_p(T_w)$ has this characteristic. Also, because of its relative insensitivity to actual surface conditions, $E_p(T_w)$ is much better than $E_p(T_s)$ as a measure of atmospheric feedbacks, which are one of the subjects of this paper.

b. Description of the climatic simulations

The climatic simulations are summarized in Table 1. Seven simulations used seven different values of soil water-holding capacity and employed a mass balance to calculate soil moisture. The conventional capacity of 15 cm (Manabe 1969) was included among these. The choices of other values were made interactively, in response to simulation results, in an effort to cover the full range of possible behavior with a small number of simulations. An eighth simulation used zero soil-water storage, hence, zero evaporation from soil; this is equivalent to a zero water-holding capacity. A ninth simulation prescribed soil-water storage at saturation, implying evaporation at the potential rate. In all other respects, the nine simulations were run under identical conditions.

All simulations began with an isothermal, resting atmosphere and no soil water. In the interactive hydrology runs, the rate of approach toward an equilibrium climate was controlled by the time scale of adjustment of soil moisture. The slowest adjustments

were at high latitudes, where the equilibrium soil moisture is near saturation and the hydrologic fluxes are small; in retrospect, spinup from a saturated state might have been more rapid. Equilibrium soil moisture was reached within 2 years in W15, and the equilibration time was approximately in direct proportion to the storage capacity in other cases. Thus, spinup durations of 4, 8, 16, and 32 yr were allowed in W30, W60, W120, and W240, respectively. A conservative spinup time of 2 yr was employed in the other simulations. The W4 and W60 simulations were continued for 10 yr of equilibrium computations; other simulations were continued for 5 yr.

c. *Description of the stand-alone land-surface simulations*

To facilitate an analysis of atmospheric feedbacks, the surface water and energy balances were also simulated, without atmospheric interactions, using algorithms extracted from the climate model. These stand-alone simulations were driven by atmospheric forcing variables that had been saved once-daily during the climate simulations. The driving variables were surface pressure, incoming shortwave and longwave radiation, solid and liquid precipitation rates, and temperature, mixing ratio, and wind speed at the lowest atmospheric level.

Four surface simulations were performed using the different possible combinations of water-holding capacity and climate associated with the W4 and W60 climatic simulations (Table 2). Each of the surface simulations was run for 15 yr, using an initial condition of dry soil, and only the last 5 yr were used for analysis. The 15-yr forcing sequence was created by cycling through the last 5 yr of the relevant climate model output (W4 or W60) three times. Simulations W4C4 and W60C60 were run as checks, and gave virtually identical outputs to the W4 and W60 climate simulations.

3. Overview of computed global water cycle and its sensitivity

The top half of Fig. 1 shows the main components in the global, annual water cycle obtained by averaging the results of W4 and W60. The cycle is similar to that obtained for W15. Annual precipitation is about 1 m over land and sea. Over land, about one-third of this amount runs off to the oceans, with a return flow by atmospheric vapor transport. The model has a small flux imbalance associated with accumulation of snow in Greenland and Antarctica. (The model has no mechanism for transporting continental ice to the ocean. This does not affect the climatic simulations, because the ocean is not interactive.) For comparison, the estimated actual water balance of the land area of the earth (Budyko and Sokolov 1978) has 75-cm precipitation, 48-cm evaporation, and 27-cm runoff; oceanic precipitation is estimated as 127 cm and evaporation as 140 cm.

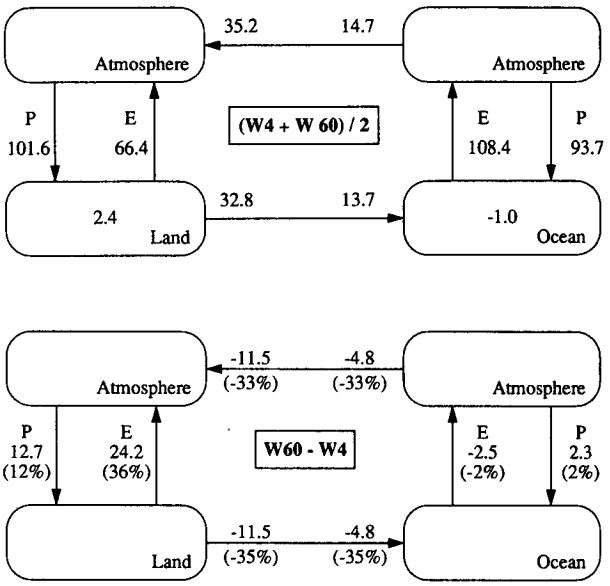

FIG. 1. Diagrams showing annual water cycle (cm yr^{-1}) for average of W4 and W60 (top) and for the difference W60–W4 (bottom). Values are equivalent volumes of liquid water per unit area of land (left) and per unit area of oceans (right). Values inside boxes give nonzero storage rates. Parenthesized values in lower diagram are percent differences relative to average of W4 and W60.

The bottom half of Fig. 1 summarizes the changes in the global water cycle between W4 and W60. (Here and elsewhere in this paper, except where explicitly noted in section 6, changes under discussion will be the differences produced by subtracting the results of W4 from those of W60; thus, they are the changes induced by changing the storage capacity from 4 cm to

TABLE 2. Summary of surface water- and energy-balance simulations.

Simulation name	Water-holding capacity (cm)	Source of forcing	Spinup duration (yr)	Equilibrium duration (yr)
W4C4	4	W4	10	5
W4C60	4	W60	10	5
W60C4	60	W4	10	5
W60C60	60	W60	10	5

60 cm.) The change in continental evaporation, about 24 cm, is split almost equally between increased continental precipitation and decreased water vapor convergence to continents (equivalently, runoff). The decreased land–ocean exchange of water is balanced by decreased oceanic evaporation and increased oceanic precipitation. In percentage terms, the changes in evaporation, runoff, and vapor flux exchange are the largest, all being over 30% of the mean of the W4 and W60 values. Continental precipitation increases by 12%.

The changes in total annual runoff (Y), evaporation (E), and precipitation (P) are mapped in Fig. 2. The larger water-holding capacity suppresses runoff and enhances evaporation over the tropical and northern midlatitude areas of the continents. The evaporation increases over all the continents; the largest changes (typically 30 to 60 cm) are in eastern South America and in much of Africa and southeastern Asia. There are also large increases (typically 20 to 30 cm) across North America, Europe, and western Asia. The changes in runoff are similar to those of evaporation, but are opposite in sign and have smaller magnitudes. At high latitudes and in eastern Asia, the runoff changes are quite small and are even variable in sign.

Because water is conserved, the sum of changes in evaporation and runoff over land equals the change in precipitation; the fact that the magnitudes of modeled changes of runoff are generally less than those of evaporation reflects the widespread increase of continental precipitation from W4 to W60. Figure 2 shows that the largest increases in continental precipitation (typically 10 to 30 cm) occur in the tropical rain belt and in the northern middle latitudes. Much of the water vapor from increased evaporation is transported to the oceans, however. Offshore transport is especially apparent in the tropics; precipitation increases throughout the equatorial oceans, with the largest additions (10–30 cm) appearing in the Atlantic and Indian Oceans.

Further details of these hydrologic changes are explored in the next two sections, which also present explanations of the physical mechanisms driving the changes.

4. Response of continental surfaces

The analysis begins with an examination of the response of the surface water balance to the change in the water-holding capacity. The effects on the surface energy balance are also briefly discussed. It will be shown that part of the surface response is caused by atmospheric feedbacks; they will be described in the subsequent section on atmospheric response.

a. Separation of direct effects and atmospheric feedbacks—Methodology

One can view runoff and evaporation changes as the sums of two components, direct and indirect. Direct changes are those that would result from the change of storage capacity in the absence of any associated change of the climate. Indirect changes reflect atmospheric feedbacks; they are the changes that would result if the storage capacity were held fixed, but the climate were changed from that of W4 to that of W60.

Let Z denote some surface water-balance variable of interest (evaporation or runoff). The quantity Z is a function of the water-holding capacity w_0 of the surface, the atmospheric forcing $\underset{\sim}{\Omega}$ at the surface (incident radiation, precipitation, and the physical state of the lowest atmospheric layer), and other surface characteristics that do not change between our simulations. Let superscripts designate the simulation from which the value of a variable is obtained. The change in Z between W4 and W60 (denoted here and elsewhere in this paper as ΔZ) may be decomposed as

$$\begin{aligned}\Delta Z = Z^{60} - Z^{4} &= Z(60, \underset{\sim}{\Omega}^{60}) - Z(4, \underset{\sim}{\Omega}^{4}) \\ &= \tfrac{1}{2}\{[Z(60, \underset{\sim}{\Omega}^{60}) - Z(4, \underset{\sim}{\Omega}^{60})] \\ &\quad + [Z(60, \underset{\sim}{\Omega}^{4}) - Z(4, \underset{\sim}{\Omega}^{4})]\} \\ &\quad + \tfrac{1}{2}\{[Z(60, \underset{\sim}{\Omega}^{60}) - Z(60, \underset{\sim}{\Omega}^{4})] \\ &\quad + [Z(4, \underset{\sim}{\Omega}^{60}) - Z(4, \underset{\sim}{\Omega}^{4})]\} \\ &= \Delta_D Z + \Delta_I Z \quad (1)\end{aligned}$$

in which $\Delta_D Z$ is the component of ΔZ that can be attributed directly to the change in water-holding capacity, and $\Delta_I Z$ is the indirect part of ΔZ that is caused by atmospheric feedbacks. The quantities in (1) were estimated using output from the stand-alone surface simulations. For example, the variable $Z(60, \underset{\sim}{\Omega}^{4})$ was evaluated using the output from the simulation W60C4.

b. Separation of direct effects and atmospheric feedbacks—Results and analysis

The seasonal and latitudinal dependences of total, direct, and indirect changes of runoff (Y) and evaporation (E) over the continents are shown in Fig. 3. The total and direct changes are very similar, and the atmospheric feedbacks are mostly of secondary importance.

1) Direct effects—Interseasonal and intraseasonal storage

In the middle latitudes, the direct effect of an increased storage capacity is a decrease in runoff during fall, winter, and (especially) spring; these are periods when water from precipitation and snowmelt tends to exceed the equivalent energy available for evaporation. Some of the water that runs off in W4 is instead stored in W60 and saved until the period of high insolation

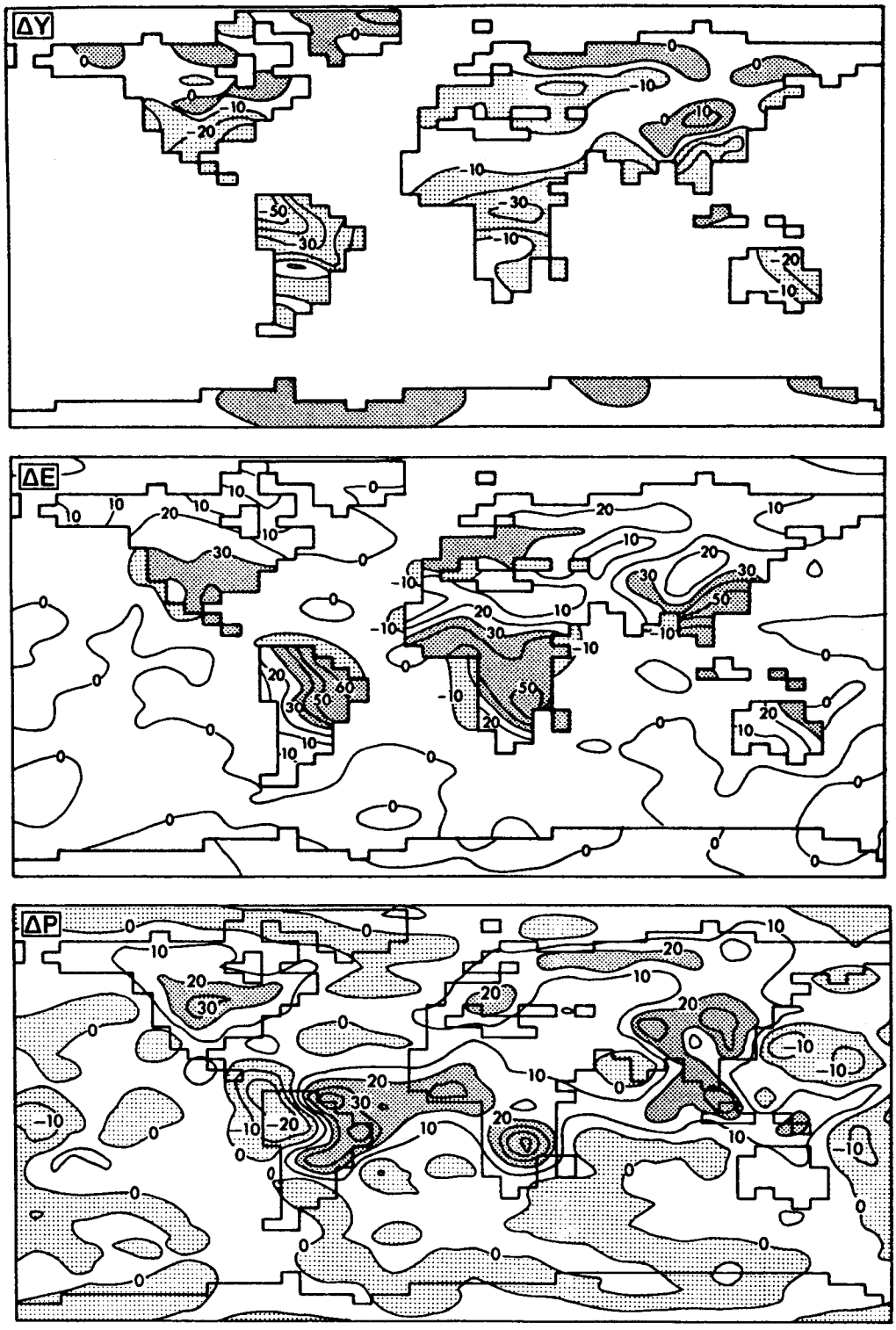

FIG. 2. Global distributions of differences (W60–W4) in total annual runoff (ΔY, top), evaporation (ΔE, middle), and precipitation (ΔP, bottom), all in centimeters.

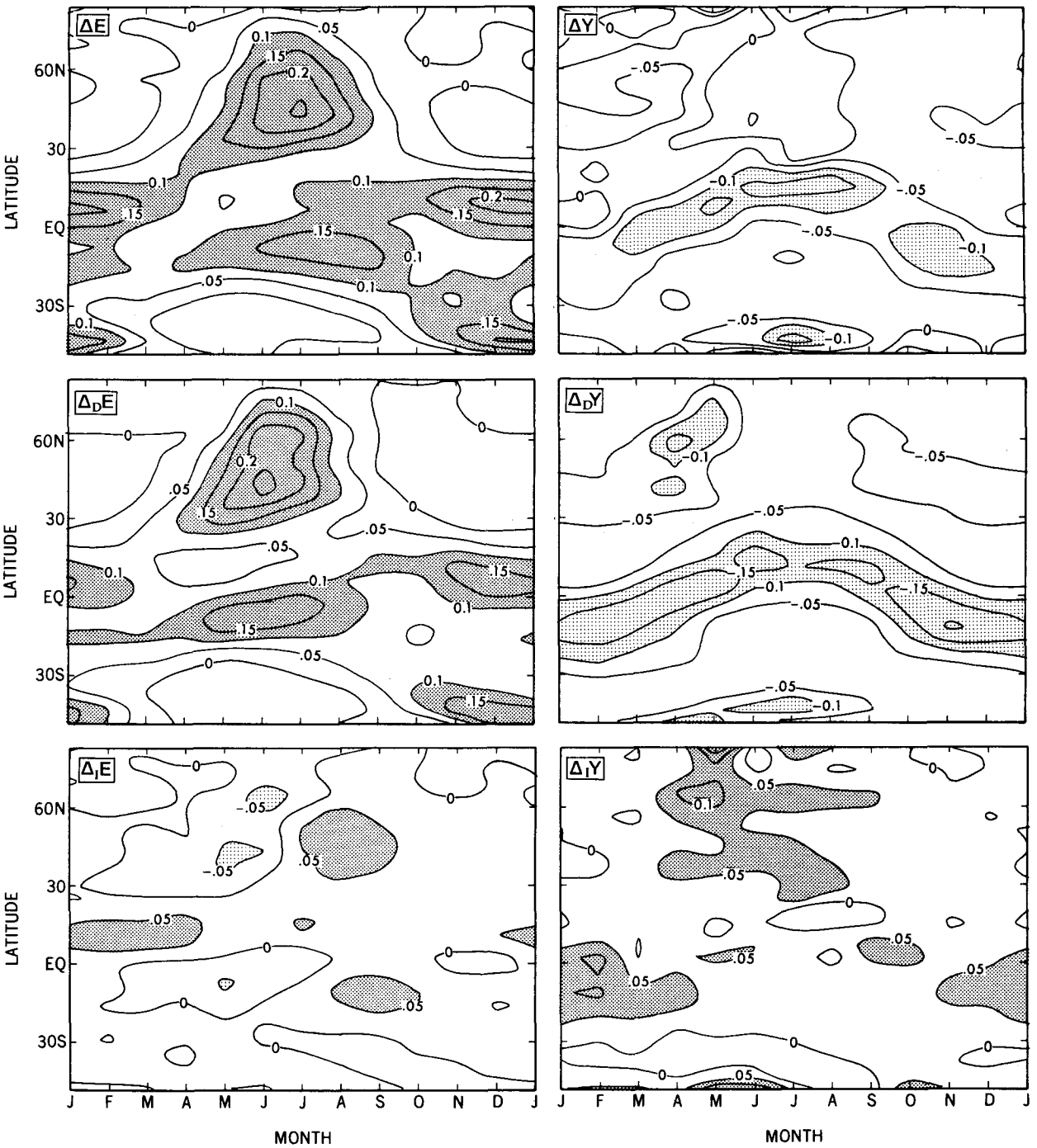

FIG. 3. Total (top), direct (middle), and indirect (bottom) differences in zonal-mean evaporation (left) and runoff (right) rates (cm d^{-1}) over continents, as function of latitude and time of year. (Note that a lower threshold is used for shading in the indirect change panels.)

during late spring and early summer, when it evaporates. (In the annual mean, direct reductions in runoff are identical to direct increases in evaporation, because their difference equals the change of precipitation, which is a climatic variable.)

A similar interseasonal storage effect is evident in the tropics, where the seasonally migrating intertropical convergence zone (ITCZ) has a water-supply excess and the bordering areas are relatively water poor and energy rich. The direct changes of runoff in the tropics

are centered on the ITCZ. In contrast, the largest tropical evaporation changes occur during the dry season.

Significant tropical increases of evaporation also occur when the ITCZ is overhead. This sensitivity of evaporation to storage capacity during a season of water excess cannot be explained simply by reference to seasonal averages of supply and demand, but is instead associated with their intraseasonal variability (Milly 1993). Water and energy supply to the surface are episodic, and there can be temporary water shortages even during a season of water excess; such a shortage occurs whenever the time between two successive rainstorms is more than long enough for water storage to be fully depleted. Similarly, dry season evaporation may be less than precipitation because of the runoff that occurs when the amount of water from some storm exceeds the storage capacity. An increase of the water-holding capacity in either of these situations reduces the probability of a soil-water drought, enhances evaporation, and suppresses runoff. An inspection of the daily water balances for selected tropical grid points confirmed that runoff caused by episodic rainfalls explained the differences in intraseasonal water balance between W4 and W60. The 60-cm capacity was always large enough to prevent such runoff, but the 4-cm capacity was not. Consistent with this, the evaporation rate during many months in the tropics in W4 was significantly less than both the precipitation rate and the potential evaporation rate. In contrast, the tropical evaporation rates in W60 always equaled (or, because of interseasonal storage, exceeded) the lesser of these two rates.

Wet season evaporation was not sensitive to storage capacity in the extratropical latitudes. Analysis of the precipitation climatology revealed that the mean amount of water delivered by an individual precipitation event was much smaller at the higher latitudes than in the tropics. Furthermore, the presence of snow cover is equivalent to an increase in the soil-water holding capacity. These two factors made temporary soil-water droughts at the higher latitudes during climatologically wet seasons extremely rare. In neither W4 nor W60 did the monthly, extratropical evaporation rates drop significantly below the lesser of the precipitation and potential evaporation rates.

2) ATMOSPHERIC FEEDBACKS

Figure 3 also shows the indirect changes of runoff and evaporation, which are caused by atmospheric feedbacks. In the tropics, runoff from the ITCZ is enhanced. The indirect changes in tropical evaporation are small on the ITCZ, but show a tendency for increases outside the ITCZ. In the northern middle and high latitudes, there is an indirect enhancement of runoff, mainly during the warm half of the year. There is also a suggestion of indirect evaporation decreases in early summer, followed by indirect increases in late summer. In the annual mean, then, and at all latitudes, the atmosphere provides a significant negative feedback to the direct changes in runoff, but only a small feedback to evaporation.

The atmospheric variables that are important for the indirect surface hydrologic changes are precipitation and potential evaporation, whose sensitivities will be described in the next section. Increased evaporation will tend to increase precipitation and to cool and moisten the lower atmosphere, leading to a decrease in potential evaporation. The increases of precipitation and decreases of potential evaporation both tend to increase runoff. On the other hand, their effects are in opposition for evaporation.

The above-mentioned factors explain the distributions of the indirect changes in Fig. 3. Indirect runoff changes are largest on the ITCZ and in the northern midlatitude summer, where both feedbacks are acting in concert. (As will be seen later, tropical increases of precipitation are centered on the ITCZ.) Indirect evaporation changes are generally weak, because of opposition of the two feedbacks. Nevertheless, the increases tend to occur where evaporation is water limited (late summer in the northern midlatitudes, and dry season in the Tropics), hence, where the precipitation feedback dominates; likewise, the small decreases of evaporation occur where it is energy limited (early summer in the north), hence, where potential evaporation feedback dominates.

3) TOTAL CHANGES

The foregoing discussions explain the gross features of the continental differences in annual runoff and evaporation mapped in Fig. 2. The evaporation changes are approximately those that would be expected on the basis of the direct effect alone. As a result of increased interseasonal and intraseasonal storage, the evaporation change is positive over land, having maxima in the areas with large annual water and energy supplies, and being relatively small where evaporation is always water-supply limited (model deserts of the Tropics and central Asia) or energy-supply limited (oceans, ice sheets, and far northern land area). The pattern of runoff differences is similar to that for evaporation, but also reflects the two atmospheric feedbacks. The runoff in low latitudes decreases. At higher latitudes (northern North America and far northern Eurasia) and over the Tibetan Plateau, the direct effect on runoff is small, because seasons of water shortage are short or absent. In such areas, the atmospheric feedbacks are large enough to reduce greatly or even to reverse the sign of the total change in runoff.

Oceanic changes in evaporation are weak, because the simulations prescribed no change in ocean surface temperature. There are notable decreases of evaporation from oceans and seas near the some of the continents, however, especially in the tropical and middle

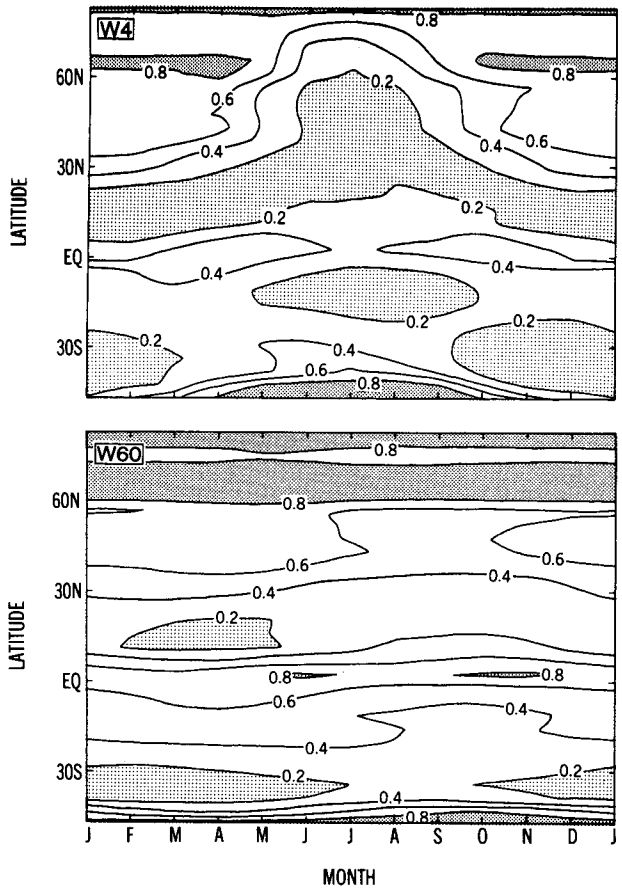

FIG. 4. Zonal-mean soil-water storage, as fraction of capacity, as function of latitude and time of year. Top: W4; bottom: W60.

latitudes. These decreases are caused by increased atmospheric humidity. This is the oceanic manifestation of the reductions in potential evaporation that have already been mentioned.

c. *Water storage*

Figure 4 shows the seasonal variations of zonal mean soil-water storage, expressed as fractions of the storage capacity. Strong seasonality is evident in the middle latitudes and in the tropics in W4; the seasonal variations are relatively small in W60. On the other hand, the actual (not normalized) seasonal changes in soil moisture are greater in W60 than in W4. The two cases represent distinct regimes in soil moisture response. With a capacity of 4 cm, the seasonal component of the storage term is insignificant in the water balance, and the time course of soil-moisture storage is determined instead by equilibrium between precipitation and soil-moisture-dependent evaporation and runoff. High values of normalized soil moisture correspond to situations where precipitation exceeds potential evaporation, and low values are roughly proportional to the ratio of precipitation to potential evaporation. With a 60-cm capacity, the storage reservoir is sufficiently large to overcome interseasonal and intraseasonal fluctuations of precipitation and potential evaporation. The interseasonal changes of soil moisture are just large enough to transfer sufficient water from the wet season to the dry season so that annual evaporation will be maximized, within the constraints of annual water and energy supply.

There is a distinct phase shift between W4 and W60, and this is associated with the different time scales of adjustment of soil water that were explained earlier. In W4, the response time is rapid, and soil-water storage is in phase with the atmospheric forcing, showing extrema at the solstices. In W60, response is relatively slow. Hence, the extrema of soil-water storage are found instead near the equinoxes; these are the times of transition from wet season to dry season.

d. *Surface energy balance*

Figure 5 shows the changes in zonal, annual means over land of the surface energy fluxes and temperatures.

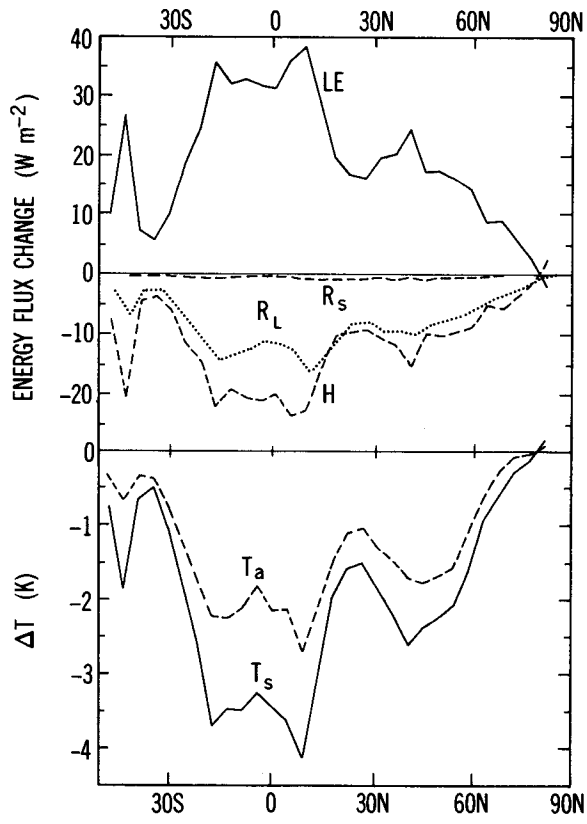

FIG. 5. Differences (W60–W4) in zonal, annual means over land of surface energy fluxes (W m^{-2}), surface temperature (T_s, K), and near-surface (σ = 0.99) air temperature (T_a, K): H is sensible heat flux; LE is latent heat flux; R_L is net longwave radiation from surface; and R_s is negative of net shortwave radiation absorbed by surface.

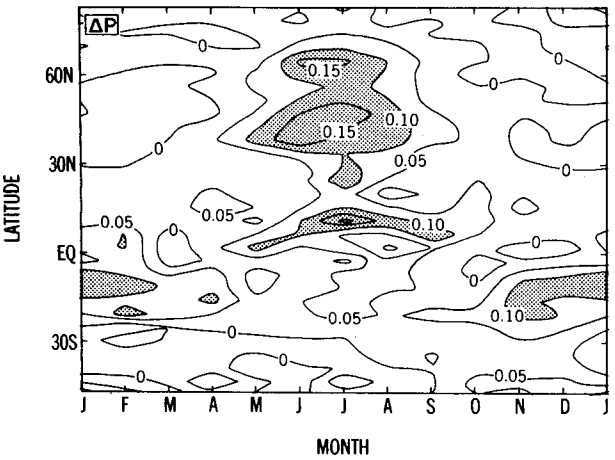

FIG. 6. Difference (W60–W4) in zonal-mean precipitation rate (cm d^{-1}) over continents as function of latitude and time of year.

The land surface is cooled by the extra evaporation in W60. This cooling is balanced by decreases in the sensible heat flux and the net loss of longwave radiation. To reach the new balance, the surface temperature must drop. In the global average over land, the annual evaporation increase of 24 cm leads to a temperature change of −2.0 K, implying a sensitivity of −0.08 K/(cm yr^{-1}) or −0.1 K/(W m^{-2}). The surface cooling is felt also in the lower atmosphere; at the lowest atmospheric layer of the model, the temperature change over land averages −1.3 K. The spatial and temporal distributions of the changes in surface energy fluxes and temperatures approximately follow the distribution of the changes in evaporation.

5. Response of atmosphere

The analysis of the surface response in the previous section indicates that a change in soil water-holding capacity causes changes in the water and heat fluxes into the atmosphere. It was also shown that the surface response was affected by atmospheric changes that affect precipitation and potential evaporation. Therefore, we begin this section with descriptions of the modeled changes of precipitation and potential evaporation. As noted in the overview already, there are significant differences between the changes in evaporation and precipitation; the analysis of the implied changes in water vapor flux convergence will be the subject of the remainder of this section. Tropical changes in diabatic heating and circulation are a major factor in the redistribution of water vapor, so special attention is devoted to these phenomena.

a. Precipitation and water vapor flux convergence

A comparison of maps in Fig. 2 showed that much of the precipitation from additional continental evaporation occurs over the oceans. A comparison of the seasonal distributions of the changes of evaporation (Fig. 3) and precipitation (Fig. 6) is also informative. Because of the short residence time of water vapor in the atmosphere, the northern extratropical increases of precipitation are contemporaneous with those of evaporation, with a maximum in early summer. In the tropics, there is a striking difference between the two distributions. The largest evaporation changes, at any time of year, fall on the edges of the ITCZ, but the contemporaneous increases of precipitation are instead centered on the ITCZ, where upward motion favors precipitation.

The transport of additional water vapor toward the oceans and toward the ITCZ can be seen clearly in Fig. 7, which shows zonal means of changes in $P-E$, with

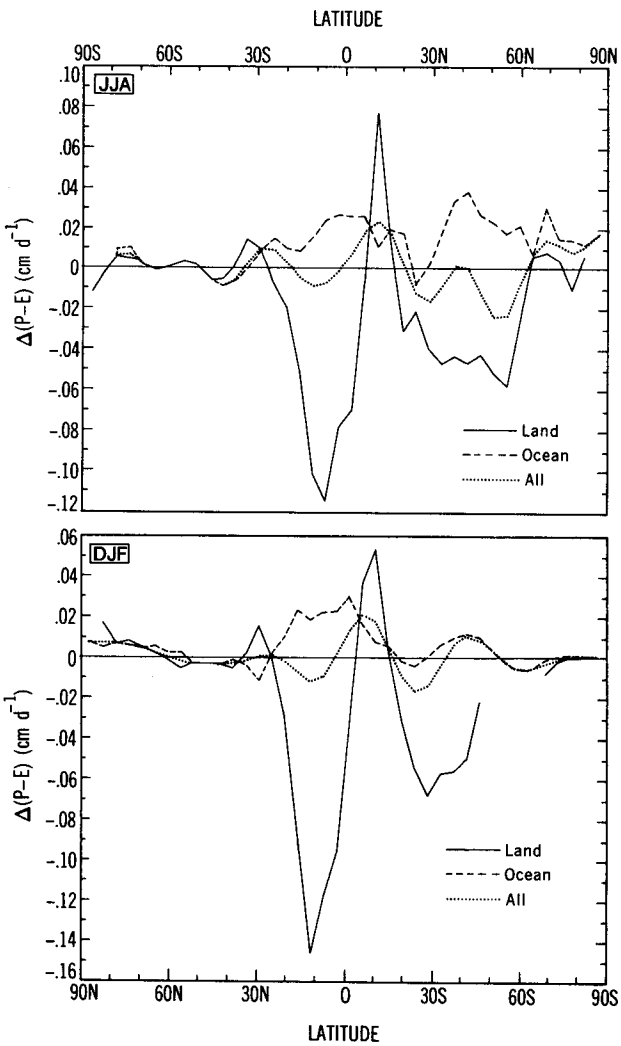

FIG. 7. Differences (W60–W4) in zonal-mean $P-E$ (cm d^{-1}) over land, sea, and all areas during June, July, and August (JJA, top) and December, January, and February (DJF, bottom). Note reversal of latitude axis for the different seasons.

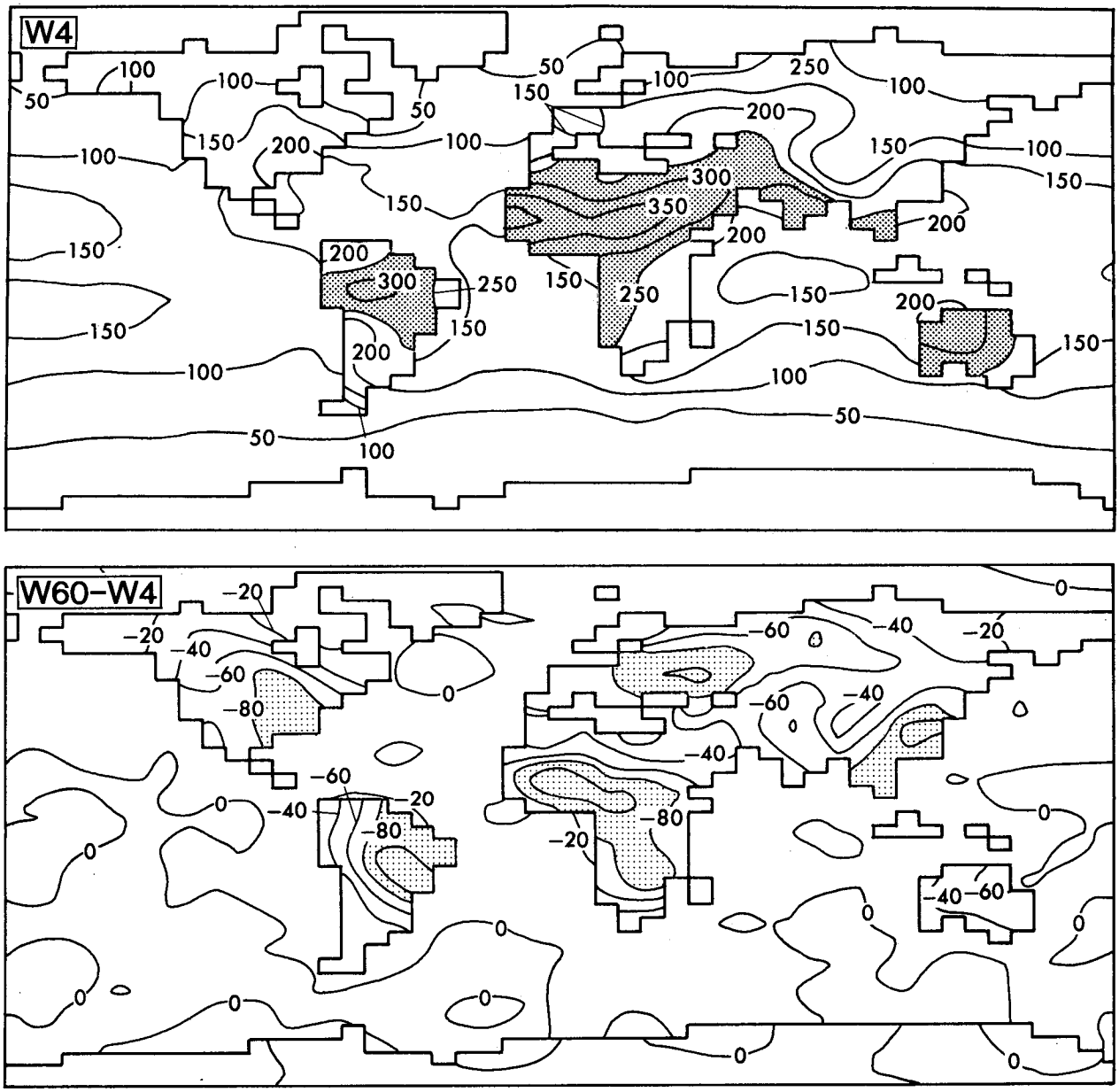

FIG. 8. Distribution of total annual potential evaporation (cm) for W4 (top) and W60–W4 (bottom).

a breakdown between land and ocean. This change in $P-E$ is essentially equal to the change in convergence of atmospheric water vapor flux. Lumping together the land and ocean surfaces, we see that there is a net change in transport of water to the ITCZ in the summer tropics (increase of $P-E$) from the winter tropics and from the summer subtropics (decreases of $P-E$). This is indicative of increased boundary-layer transport of water vapor associated with the Hadley circulation.

Superimposed upon the increase of meridional transport in the tropics is a zonal transport of water from continents to oceans, also visible in Fig. 7. This is strongest in the winter hemisphere, and is reversed only in a narrow band at the ITCZ. Decreased onshore transport of water vapor in the tropics is suggestive of a reduction in boundary-layer transport of water vapor associated with monsoon circulations. Figure 7 also shows a zonal transport of water vapor from land to ocean in the middle latitudes in summer.

b. Potential evaporation

The calculated potential evaporation in W4 and the difference between W60 and W4 are shown in Fig. 8.

In W4, values over land generally increase from the poles to low latitudes, and show increases with aridity at a given latitude. Examples of the latter feature include Australia, the Sahara, and Kazakhstan, all of which receive little precipitation in W4. The distribution of potential evaporation can be understood in terms of Penman's (1948) expression for evaporation from a water surface, which shows that potential evaporation is a weighted average of the net radiation (expressed as an equivalent evaporation rate) and a quantity identified as the drying power of the air, the latter being directly proportional to the deficit of the near-surface humidity below its saturation value. The net radiation term explains the equatorward increase of values, and the drying power term explains the elevation of values in arid regions.

In W60, there is a marked decrease in potential evaporation over land relative to W4 (Fig. 8), which is caused mainly by reduction in the drying power of the air in W60. This comes about as a result of the humidification and cooling of the atmosphere in those regions experiencing increases of evaporation or vapor convergence.

c. *Atmospheric heating and the tropical circulation*

1) HEATING PROFILES

As seen earlier, the surface cooling caused by increased evaporation in W60 relative to W4 is transmitted to the lower atmosphere. Cooling of the lower atmosphere is transmitted further upward by reductions in upward heat transfer by convective overturning. This cooling is opposed by condensational heating from the additional precipitation. The sum of these effects yields a change in the vertical distribution of diabatic heating of the atmosphere. Vertical profiles of changes in the various heating terms were analyzed in detail. The analysis revealed that the model atmosphere is highly efficient at transporting heating changes from the surface upward through the troposphere, mainly by changes of convective adjustments. In fact, convection is so intense in the model that the net change in the diabatic heating profile resulting from a given increase of precipitation is similar (but of opposite sign) to that resulting from an equal increase of evaporation at the surface. This equivalence of precipitation and evaporation simplifies the analysis of the effects of changes in heating on the model circulation. In what follows, we shall restrict our attention to the vertical integral of diabatic heating.

2) VERTICAL INTEGRAL OF HEATING

To simplify the presentation in this section, we shall ignore the heat of fusion of water; this does not significantly change the results. The total diabatic heating Q of a column of atmosphere is composed of radiative, sensible, and latent terms,

$$Q = R_{ToA} - R_{sfc} + H + LP \tag{2}$$

in which R_{ToA} and R_{sfc} are all-wave downward radiation fluxes at the top of the atmosphere and at the surface, H is sensible heat flux from the surface, L is latent heat of condensation, and P is the precipitation rate on a mass basis. The surface energy balance equation is

$$R_{sfc} = LE + H + G \tag{3}$$

in which G is the heat flux into the underlying land or ocean. Combination of these yields

$$Q = R_{ToA} + L(P - E) - G. \tag{4}$$

In our experiment, G is set to zero over land and changes comparatively little over ocean. Likewise, changes in R_{ToA} are small and balance G globally. The dominant changes in Q are therefore associated with changes in P–E,

$$\Delta Q \approx L\Delta(P - E). \tag{5}$$

The patterns of zonal changes in solstitial diabatic heating may therefore be inferred from Fig. 7. There is increased heating of the ascending branch of the Hadley cell and decreased heating of the descending branches. Superimposed upon this are a reduction in heating over the tropical continents and an increase over the oceans. The land–ocean change also occurs in summer in the extratropics.

In view of the relation between heating and atmospheric dynamics, it is reasonable to expect circulation changes in response to the heating changes. The connection between heating, Q, and circulation can be seen in the vertically integrated, steady-state form of the thermodynamic energy balance equation,

$$\int_0^1 (\mathbf{v}_H \cdot \nabla_H T)\, d\sigma + \int_0^1 (-\omega S)\, d\sigma = \frac{gQ}{c_p p^*}, \tag{6}$$

in which the subscript H denotes the horizontal component of a vector, p^* is the surface pressure, $\mathbf{v}$ is the wind, ω is the pressure velocity, and S is the stability defined by

$$S = \frac{RT}{c_p p} - \frac{\partial T}{\partial p}. \tag{7}$$

In the tropics, heating is typically balanced by changes in vertical heat transport and conversion to kinetic energy ($-\omega S$), so a correspondence between the fields of pressure velocity and heating is to be expected; at higher latitudes, adjustments in horizontal advection ($\mathbf{v}_H \cdot \nabla_H T$) dominate the response to changes of heating (Held 1983). In what follows, we shall see how the changes in heating lead to changes in tropical circulation.

3) HADLEY CIRCULATION

The zonal mean, over land and ocean, of the change in Q is shown in the upper panel of Fig. 9. Consistent

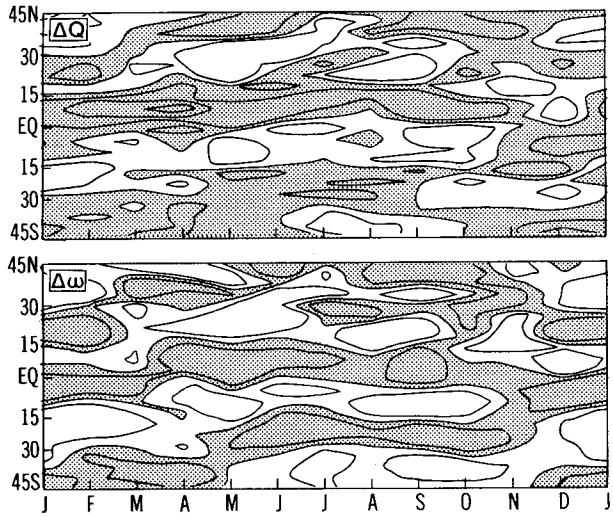

FIG. 9. Top: difference (W60–W4) in zonal-average diabatic heating rate, Q, as function of latitude and time of year. Contour interval is 4 W m^{-2}, and positive values are shaded. Bottom: same for difference in pressure velocity, ω, at $\sigma = 0.83$. Contour interval is 10^{-6} kPa s^{-1}, and negative values are shaded.

with Fig. 7, the pattern is one of increased heating on the ITCZ and relative cooling on its fringes, with magnitudes on the order of several watts per square meter. Also plotted in Fig. 9 is the change of pressure velocity, ω, at $\sigma = 0.83$ (about 1500 m above the surface) in the model; a decrease of ω indicates increased upward motion. The intensification of the Hadley circulation is apparent.

The similarity of the changes in heating and vertical motion is indicative of a strong physical link between the two. In part this is attributable to the diabatic forcing of circulation given by (6). However, there are also strong positive feedbacks, in that the increased convergence (divergence) and upward (downward) motion enhances (inhibits) precipitation and, to a certain extent, reduces (increases) the drying power of the air, and hence evaporation. The changes of circulation therefore act to amplify the hydrologic changes that would have occurred with a fixed circulation.

4) LAND–OCEAN CIRCULATION

The upper panel in Fig. 10 shows the change in annual diabatic heating; this is essentially the change in P–E, converted to energy units. The tropical land–ocean heating contrast is striking. Relative cooling of more than 10 W m^{-2} occurs over land in the tropics, where increases in precipitation are less than increases of evaporation. Relative heating of similar magnitude occurs over the tropical oceans. Differential cooling also occurs over southeast Asia, southern North America, and eastern Australia, with associated heating increases over adjacent ocean areas.

The lower panel in Fig. 10 shows the change in the pressure velocity at $\sigma = 0.83$. The similarity of the heating and motion fields is striking. Relative rising (sinking) is associated with relative heating (cooling).

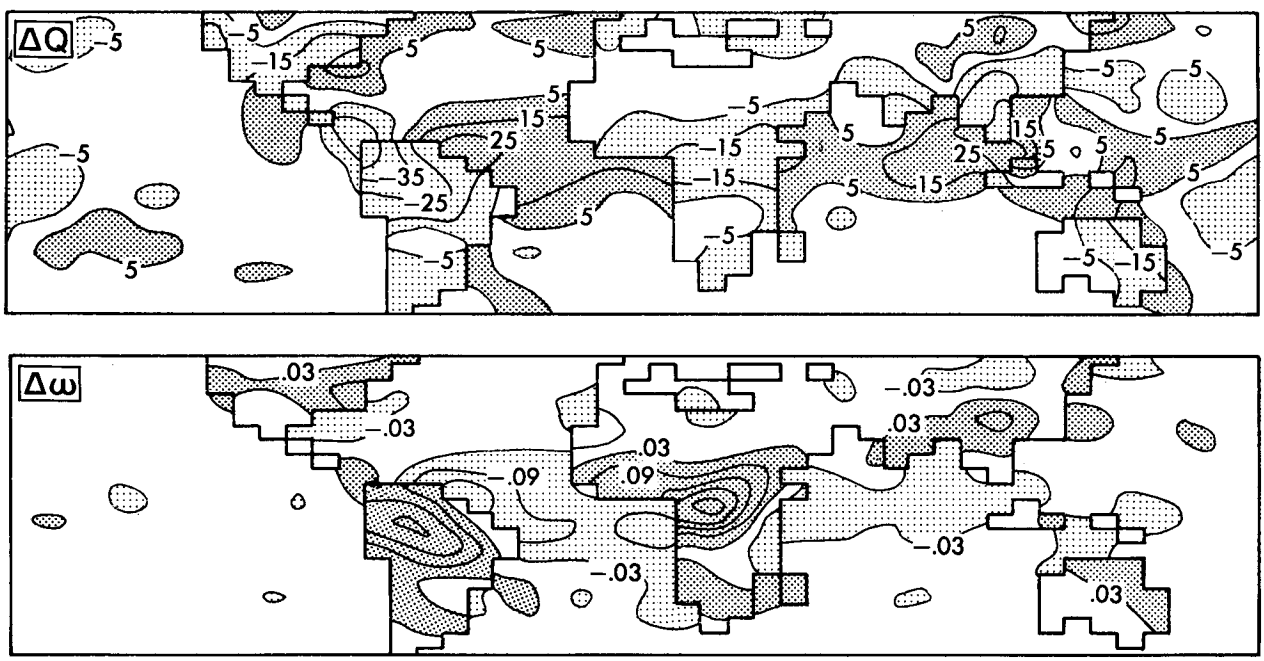

FIG. 10. Top: distribution of difference (W60–W4) in annual-mean diabatic heating rate, Q (W m^{-2}). Bottom: same for pressure velocity (10^{-6} kPa s^{-1}) at $\sigma = 0.83$.

The strongest changes of vertical motion occur in equatorial South America and Africa. Extratropical changes of vertical velocity are relatively small, but well correlated with the heating changes. Associated with the tropical changes of vertical velocity are near-surface wind changes that are directed offshore from continental areas of relative sinking to oceanic areas of relative ascent. These changes are particularly strong near the equatorial Atlantic coasts of South America and Africa.

As in the case of the Hadley circulation, the heating changes and monsoonal circulation changes are mutually reinforcing. The heating changes tend to reduce the prevailing ocean–land heating contrast, thereby reducing the intensity of the monsoon circulations. In turn, this reduces the onshore transport of water vapor, thereby amplifying the heating perturbations. The main mechanism initiating this change in the monsoons can be understood in terms of water vapor advection by the prevailing circulation. Due to the change in soil water-holding capacity, evaporation increases over the continents. Some of the air moistened over the continents inevitably travels to the oceans, where the additional vapor condenses as precipitation. There would, therefore, be a net decrease in onshore transport of water vapor even in the absence of circulation changes.

d. Mechanisms of water vapor transport

1) WATER VAPOR TRANSPORT

A water balance on a full atmospheric column of air can be expressed

$$\frac{\partial w}{\partial t} = -g^{-1}\nabla_H \cdot \int_0^1 (p^* \mathbf{v}_H q)\, d\sigma + E - P, \quad (8)$$

in which w is total precipitable water, p^* is surface pressure, $\underset{\sim}{v}$ is wind velocity, and q is water vapor mixing ratio. Taking the expectation (denoted by angle brackets), and neglecting the storage term, which is small throughout the year, we have

$$\langle P - E \rangle = -g^{-1}\nabla_H \cdot \int_0^1 \langle p^* \mathbf{v}_H q \rangle\, d\sigma. \quad (9)$$

To an excellent approximation, the difference in balances between two simulations (denoted by Δ) may be decomposed as

$$\Delta\langle P - E \rangle = -g^{-1}\nabla_H \cdot [\langle p^* \rangle] \int_0^1 \Delta(\langle \mathbf{v}_H \rangle \langle q \rangle)\, d\sigma$$

$$- g^{-1} \quad \nabla_H \cdot \langle p^* \rangle \int_0^1 \Delta\langle \mathbf{v}_H q \rangle - \langle \mathbf{v}_H \rangle \langle q \rangle\, d\sigma$$

$$= \Delta_m C + \Delta_e C \quad (10)$$

in which square brackets denote a mean of the two climates and Δ denotes their difference. The quantity $\Delta_m C$ is the change in convergence of water vapor flux carried by the mean wind, including components associated with the changes in the mean circulation and the changes in the mean humidity. The remaining changes, $\Delta_e C$, are changes in transient eddy fluxes of water vapor.

Figure 11 shows zonal, annual means of the differences of total convergence of atmospheric water vapor flux, along with the individual components $\Delta_m C$ and $\Delta_e C$. The top panel is the annual mean version of Fig. 7, showing clearly the zonal transfer, at all latitudes, of water from the atmosphere above the continents to the atmosphere above the oceans and the intensification of meridional water cycling associated with the Hadley circulation.

The second and third panels in Fig. 11 show the components of the changes in convergence. In the

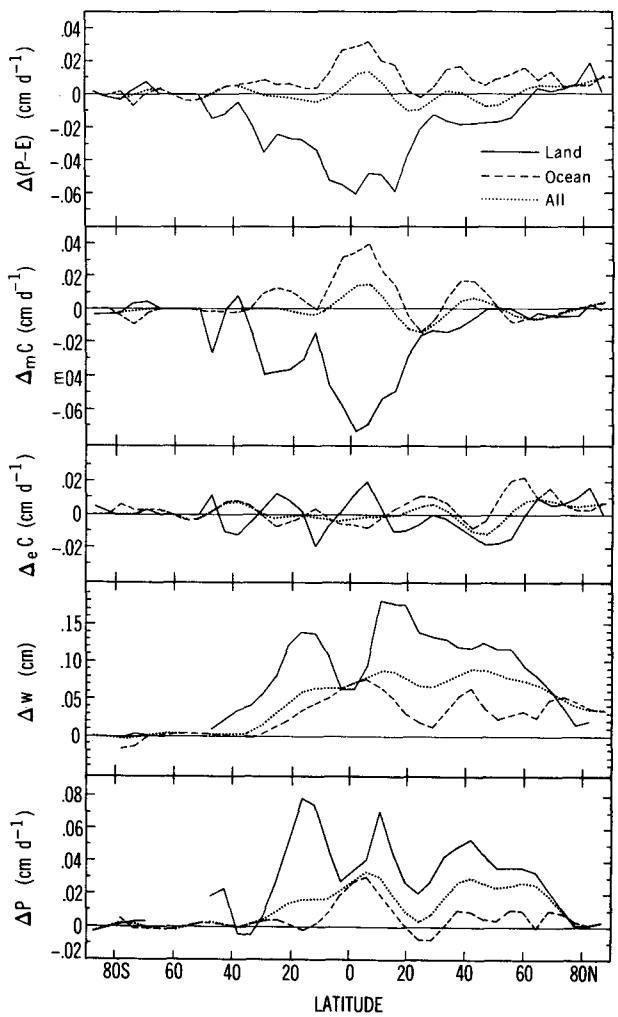

FIG. 11. Differences in zonal annual means, over land, oceans, and all area, of convergence of horizontal water-vapor flux (P–E, cm d^{-1}) and its components ($\Delta_m C$, $\Delta_e C$, cm d^{-1}), vertically integrated water vapor content of atmosphere (w, cm), and precipitation (P, cm d^{-1}).

tropics and as far north as 40°N, the change in advection of water vapor by the mean wind is dominant; this is a result of the strong tropical circulation response that has already been discussed. Further partitioning of the change in advection into its components due to wind changes and humidity changes revealed that the wind changes were dominant.

North of 45°N, the effect of transient eddies dominates. Changes in transport due to transient eddies can also be seen in the tropics. There is a net convergence over land in a narrow band centered just north of the equator, which is the location of the center of the annual mean ITCZ, and divergence over land in the adjacent latitude belts. A brief analysis of the changes in transient eddy fluxes of water vapor is presented next.

2) HUMIDITY AND TRANSIENT EDDY TRANSPORT OF WATER VAPOR

If the kinetic energy of transient eddies remains relatively unchanged, then the changes in transient eddy flux ought to be associated with changes in the gradients of mixing ratio of water vapor. The fourth panel in Fig. 11 shows the changes in vertically integrated water content w of the atmospheric column, for land and ocean separately. Also shown, in the bottom panel, are the changes in precipitation. The humidity changes are driven primarily by the increase of the intensity of water cycling; an increased water content of the air is necessary to maintain an increased precipitation rate. This concept is supported by a comparison of the zonal means of changes in precipitation (bottom panel) and precipitable water, which show very similar patterns. Generally, the moistening over continents exceeds that over oceans. In a narrow band centered just north of the equator, where the difference between precipitation changes over land and ocean is negligible, the change in the sea–land humidity contrast is also insignificant.

The decreased sea–land humidity differences explain the reduced onshore transient eddy transports of moisture. On the equator, where zonal average humidity changes do not differ between land and sea, the eddy flux over land actually reverses sign. Here the positive contribution of transient eddy fluxes to $P-E$ is caused by the meridional gradients of w over land, which are tending to drive moisture toward this differentially dried region.

6. Overview of results from all simulations

In the last two sections, we have analyzed the differences between simulations using soil water-holding capacities of 4 cm and 60 cm. In this section we present a less intensive comparison of all nine simulations. The main objective here is to explore the limits of small and large capacities and the nature of the transition between these limits. We concentrate on the global means of evaporation, but also mention the global means of other selected variables and the meridional distribution of the components of the surface water balance.

a. Global means

Figure 12 shows the annual evaporation and precipitation averaged over all land for all nine simulations; the difference $P-E$ is approximately equal to the runoff. The DRY simulation is equivalent to a zero-storage capacity simulation; in this case, evaporation from the continents (6.6 cm) occurs only as sublimation of snowpack. At the other extreme is the SAT simulation, in which evaporation (102.8 cm) is allowed to occur at the potential rate. The DRY and SAT simulations represent the extreme limits of hydrologic behavior of the continental surfaces. These two simulations correspond to the dry and wet simulations of Shukla and Mintz (1982).

In the simulations with interactive soil moisture, the amounts of evaporation lie within the bounds set by DRY and SAT. As storage capacity increases from zero, evaporation also increases, but beyond a certain point there is no further sensitivity of evaporation to storage capacity. This point corresponds to the situation discussed in the Introduction, wherein all temporal fluctuations of precipitation and potential evaporation are overcome by the storage capacity. This "saturation" of the storage effect occurs in these experiments only asymptotically; the W60, W120, and W240 simulations are very close to this limit. The global evaporation at this limit is far short of that in the SAT climate, because the latter has evaporation in excess of precipitation over extensive arid regions, whereas the other simulations have a local water balance.

The precipitation changes shown in Fig. 12 follow those of evaporation, but with less sensitivity. Only

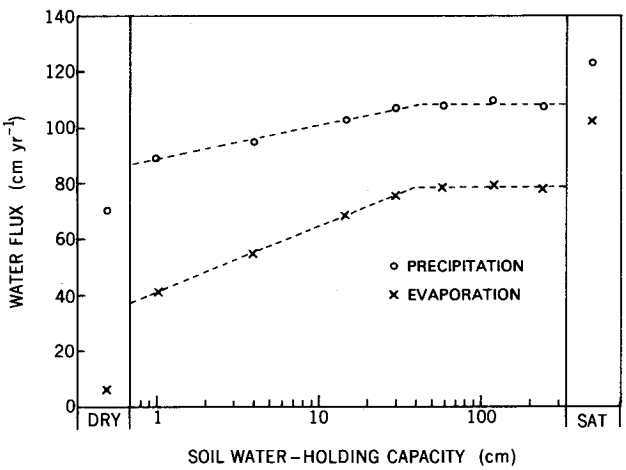

FIG. 12. Annual evaporation and precipitation (cm yr^{-1}), averaged over all land areas, for each simulation.

about half of the change in evaporation between simulations is returned to land; the rest is effectively transported to the oceanic part of the atmosphere.

Even a small storage capacity contributes much to an increase in evaporation above that in the DRY case. For example, 1 cm of capacity increases the annual evaporation by 35 cm over that with no capacity. This is the result of repeated filling of the storage capacity by precipitation and subsequent emptying by evaporation throughout the year, in connection with the intraseasonal storage process. It is remarkable that a mere centimeter of capacity is about half as effective as an arbitrarily large capacity in producing evaporation from the continents. Returns diminish as the capacity is progressively increased; in the region of sensitivity to storage capacity, a doubling of capacity is needed for each 7-cm increase in evaporation.

Global mean values of several important climatic variables were found to be almost in direct proportion to the mean evaporation across these experiments, even for the markedly different SAT case. It may be inferred that the detailed physical analyses of changes presented in earlier sections of this paper apply, at least in a gross sense, to the full range of experiments. Of course, there are some differences in the geographic distributions of changes.

b. Meridional distributions of changes in water balance

The zonal-mean, land-only differences in evaporation, precipitation, and runoff for W1-DRY, W4-W1, W60-W4, and SAT-W60 are shown in Fig. 13. All fluxes are normalized by the corresponding global-mean difference in evaporation from land to facilitate comparison of the responses. In all cases the dependences of precipitation and runoff changes on the evaporation changes are consistent with those identified in earlier sections of this paper. The sensitivities for the first three pairs of simulations are broadly similar; the major difference is in the tropics, where the evaporation sensitivity peaks near the equator for low values of storage capacity, and has a broader profile at higher values. In the limit of small capacity, it is to be expected that the change in evaporation will be proportional to the number of storm events; this is maximized at the annual average center of the ITCZ. As the storage capacity is increased, the storage effect "saturates" on the wet ITCZ, but is still important for the relatively dry fringe areas.

The zonal distributions of changes for SAT-W60 are markedly different from the others. The dominant feature is the increase of evaporation from normally dry subtropical deserts.

7. Summary and discussion

In this section, we summarize the main findings from the numerical experiments. We then speculate on the

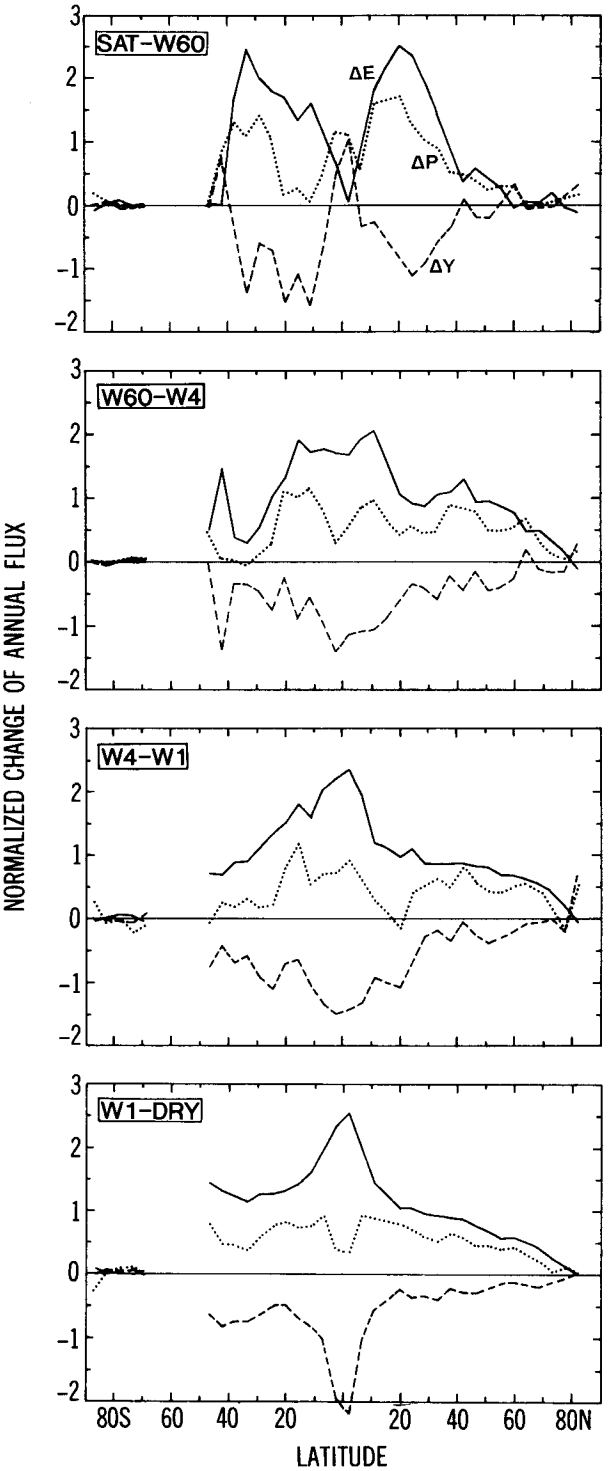

FIG. 13. Zonal-mean, land-only differences in total annual evaporation, precipitation, and runoff for various pairs of simulations. All values are normalized by the global-mean difference in total annual evaporation over land.

implications of this study for various problems in climate dynamics. Finally, we note some of the limitations of the study.

a. Summary

The sensitivity of the global water cycle to the effective water-holding capacity of the plant-root zone of continental soils was estimated by simulation. The simulations used a climate model that included a model of the general circulation of the atmosphere coupled to a simple water-storage model for the continental surfaces. Ocean surface temperatures and clouds were prescribed. Equilibrium climates were computed for each of seven values of a globally constant soil-water-holding capacity (1, 4, 15, 30, 60, 120, 240 cm), and for completely dry and moist continental surfaces. Detailed analyses were made of the differences between the 4- and 60-cm cases, and brief comparisons of all simulations were made to establish the generality of the results.

With an increase of the storage capacity, evaporation from the continents rose and runoff fell, because a high storage capacity enhanced the ability of the soil to store water from periods of excess for later evaporation during periods of shortage. Most of the changes in evaporation and runoff occurred in the tropics and in the northern middle-latitude rain belts. The global evaporation from land varied linearly with the logarithm of the storage capacity; evaporation increased by about 7 cm for each doubling of storage capacity in the range from 1 cm to almost 60 cm. The 60-cm storage capacity was large enough to balance virtually all temporal fluctuations in the surface water and energy supplies that determine evaporation at a given location; there was little sensitivity to storage capacities above this value. The global, annual mean values of other climatic variables varied almost linearly with evaporation across the various simulations.

Evaporation and runoff were also affected by atmospheric feedbacks. These were associated with the increase of precipitation and decrease of potential evaporation that arose when evaporation increased. A series of stand-alone simulations of surface water and energy balances was run to separate the direct effects from the atmospheric feedbacks. These simulations showed that both the precipitation and the potential evaporation feedbacks tend to increase runoff, but their effects on evaporation tend to cancel each other. The analysis also showed that the atmospheric feedbacks are of secondary importance in comparison with the direct effects.

Increased cooling by evaporation affected the surface energy balance. Global-average land-surface temperature was 2.0 K lower with a water-holding capacity of 60 cm than with a capacity of 4 cm. This amount of cooling was associated with a 24-cm increase in evaporation.

Increased evaporation from continental surfaces in the tropics caused an increase in the amount of water carried by the Hadley circulation. The associated change in the meridional flux of water vapor was reflected in a change of heating of the atmosphere, which was shown to be directly proportional to the convergence of the flux of water vapor. The change of heating led to an intensification of the Hadley circulation, with a strong positive feedback to the vapor flux convergence. Increased humidity over the continents in the tropics also led to differential offshore advection of water vapor by the prevailing circulation. The associated reduction of the heating contrast between land and sea weakened the monsoonal circulations, with attendant positive feedback to decreased continental vapor flux convergence. The reduction of onshore flux of water vapor caused the increase in precipitation over the continents to be significantly less than the evaporation increase, and the precipitation onto the oceans to increase. These responses were also apparent in southern parts of the northern middle-latitude rainbelt.

The dominant factor affecting changes of water vapor transport in the northern middle latitudes was the change in transport by transient eddies. The differential moistening of the atmosphere above the continents exceeded that above the oceans. The resulting change in the sea–land humidity difference caused less water vapor to be transported to the continents by the transient eddies. This mechanism exported part of the additional moisture to the oceans, causing continental precipitation increases to be less than the evaporation increases.

b. Implications for climate sensitivity to human water use

The major direct hydrologic effect of human water use on the global water cycle is to promote the evaporation into the atmosphere of a portion of the water that would otherwise run to the oceans in the rivers of the world. This is accomplished primarily through the capture and diversion of surface runoff for irrigation of agricultural fields. Of an estimated 47 000 $km^3\ yr^{-1}$ natural runoff from the continents, in 1990 an estimated 2050 $km^3\ yr^{-1}$ was artificially returned to the atmosphere by irrigation, and the total increase of evaporation due to irrigation, industrial and municipal water use, and evaporation from artificial reservoirs was estimated as 2360 $km^3\ yr^{-1}$ (Shiklomanov and Markova 1987, p. 77); most of this occurs in the Northern Hemisphere.

In terms of this paper, water use by humans has the same effect as an increase in the water-holding capacity of land. One may use the numerical experiments described here to obtain an extremely crude estimate of the global climatic sensitivity to current human water use. Such an estimate ignores both the dependence of the mean response on the spatial distribution of the forcing and the possible cloud and ocean feedbacks.

Recognizing these caveats, we may estimate the sensitivity by scaling the W60–W4 simulation results. The 24-cm increase of annual evaporation from land in the numerical experiment amounts to 36 000 $km^3\ yr^{-1}$, or about 15 times the change given by Shiklomanov and Markova (1987). According to Fig. 1, this would be split approximately equally between increased continental precipitation and decreased water-vapor flux convergence. This implies that current levels of water use by humans drive a global precipitation increase over the continents of about 0.8 cm and a global mean air temperature drop of about 0.1 K over land. Given the concentration of the anthropogenic evaporation changes in certain areas, the local responses could also be concentrated, hence, much larger regionally. If half of the added moisture were recycled as precipitation over Eurasia and North America, then the average increases of precipitation there would be 1.5 cm and the temperature drop would be 0.2 K. These figures would appear to be further amplified when cloud feedbacks are considered; the results of a preliminary analysis of the effects of cloud changes are given near the end of this section.

Empirical estimates of trends in precipitation during the last century contain the effects of consumptive water use and other anthropogenic forcings, natural variability, and biases due to instrumental and sampling changes in the measurement network. The latter errors complicate the interpretation of trends (Intergovernmental Panel on Climate Change 1990, p. 220); the increasing efficiency of precipitation collectors and improved corrections for undercollection and evaporative losses from gauges could contribute to an increase in apparent precipitation. For 1891–1986, Vinnikov et al. (1990) have estimated precipitation trends of 3.5 cm $century^{-1}$ for the former USSR (for which they attempted to remove instrumental and operational biases) and 3.4 cm $century^{-1}$ for all land between 35°N and 70°N, excluding Canada north of 55°N. They argued that only a small part (0.5 to 1.0 cm $century^{-1}$ for the larger region) of the apparent precipitation trends could readily be explained by an assumed enhancement of the greenhouse effect. It is intriguing to consider the possibility that some significant fraction of the additional 2.4 to 2.9 cm $century^{-1}$ may be explained by an enhancement of precipitation due to consumptive water use in the Northern Hemisphere.

The climate associated with the limit of large water-holding capacity has an interesting physical interpretation. It represents a world in which water resources have been fully "developed" locally in the sense that, through the widespread use of water storage reservoirs, virtually no runoff is allowed to discharge from a particular region unless evaporation is always at the potential rate there. Given the water-use figures cited above, such a situation would be reached upon a 20-fold increase in current water use.

An interesting physical interpretation can also be given to the SAT climate. It represents a world in which water supply is everywhere sufficient to satisfy the potential evaporation. Such a situation could come about by some combination of increased reservoirs, large-scale interbasin water transfers, and large-scale desalinization and redistribution of ocean water.

c. Implications for natural selection of vegetation and soil water-holding capacity

Actual evaporation from the continents of the earth is about 65% of precipitation, so W15 is hydrologically the simulation most representative of the earth. The storage capacity of 15 cm is remarkably close to the point where the storage effect reaches saturation; the difference in evaporation between W15 and DRY is approximately 85% of the difference between W120 and DRY. It is interesting to speculate on the ecological significance of this. Plants that are resistant to water stress have an advantage over those that are not, and a major factor in the minimization of water stress is the existence of a large water-holding capacity. The capacity can be affected by the plants through their root growth and their contribution to soil structure. One might speculate that vegetation evolves or adjusts to increase storage capacity as long as it receives a significant return on investment. The progressive increase of evaporation with water-holding capacity seen in Fig. 12 represents decreasing plant water stress. Absolute minimization of stress is approached only asymptotically, and it would be expected that an optimum would exist somewhere short of that limit. The fact that the earth operates near the limit is suggestive of the importance of plant water stress in determining the water-holding capacities of the continents. This hypothesis is similar in principle to that of Eagleson (1978), but differs fundamentally regarding mechanisms.

d. Implications for climate sensitivity to large-scale soil and vegetation changes

The water-holding capacity of soils is largely a function of the depth of rooting of vegetation and the depth and physical properties of the soils (Patterson 1990). Large-scale changes in vegetation can potentially lead to large-scale changes in storage capacities of the continents, with consequences estimated in this paper. Other surface characteristics would vary in conjunction with the water-holding capacity, most notably the surface albedo and the surface roughness length, because these are also dependent on the vegetation cover. Nevertheless, it is possible to discuss the marginal effect of capacity changes in isolation.

Three numerical studies (Dickinson and Henderson-Sellers 1988; Lean and Warrilow 1989; Shukla et al. 1990; and Nobre et al. 1991) have investigated the effects on regional climate of a conversion of the Ama-

zonian tropical forests to grasslands. Significant changes in precipitation, evaporation, and runoff were noted. In all studies, the surface response was parameterized using more detailed physical descriptions of the soil and vegetation than the simple storage reservoir used in this paper. However, it is possible to make crude estimates of the implied water-holding capacities. Simple calculations of soil drainage rates based on the theory of soil-water transport suggest that the effective water-holding capacity of the root zone is almost directly proportional to the depth of rooting and depends only weakly on soil texture. On the basis of this, it is estimated that the water-holding capacity was reduced by factors of 1.5, 2.1, and 3.3 by Dickinson and Henderson-Sellers (1988), Lean and Warrilow (1989), and Nobre et al. (1991), respectively.

Assuming that all hydrologic changes are proportional to the change of the logarithm of the water-holding capacity, we may estimate what would have happened in the present model if these reductions in capacity had been imposed globally; ignoring the remote effects, this would approximate the regional response to an Amazonian deforestation. Accordingly, the deforestation effects were estimated by scaling the W60–W4 differences by factors of −0.15, −0.27, and −0.44. The resulting estimates of changes in evaporation ranged from 28% to 32% of the corresponding total changes reported by the various investigators. The estimated runoff changes were 28%, −61%, and −120% of the reported total changes. The estimated precipitation changes were small compared to the reported changes.

These results suggest that the reduction in soil water-holding capacity accompanying deforestation in numerical experiments contributes significantly to changes in evaporation and runoff (hence water vapor flux convergence). Its effects on runoff are probably opposed to the effects of the increased albedo and decreased roughness of the surface (Lean and Warrilow 1989). Furthermore, our estimates of the role of storage capacity vary by a factor of 3 among those experiments, primarily because different investigators made different assumptions about the changes in rooting depth of vegetation that accompany deforestation. It can be concluded that uncertainty in the change of factors affecting water-holding capacity leads to significant uncertainty in the climatic response to tropical deforestation.

e. Implications for sensitivity of modeled climates to hydrologic parameterization

On the basis of the results presented here, one can make inferences about the sensitivity of a climate model to its continental hydrologic parameterization. If one could identify a single parameter characterizing the hydrologic response of a land area, independent of its radiative and turbulent transfer characteristics, that parameter would probably quantify the ability of the soil and vegetation to retain water for later release as evaporation. This hydrologic "thriftiness" would depend not only on water-holding capacity of the root zone of soil water but also on the interception capacity of the vegetation, the permeability and other hydraulic characteristics of the soil, the physiological characteristics of the vegetation, and the subgrid variability of these factors. Such a simple hydrologic analog to albedo and surface roughness length cannot be easily defined, but a water-holding capacity that takes into account soil and vegetation characteristics comes close.

We suggest that the most significant feature of a hydrologic parameterization for large-scale problems in climatic modeling is its hydrologic thriftiness. High thriftiness implies ability to store large amounts of water over various periods of time, and results in maximum evaporation and minimum runoff for given atmospheric conditions and surface radiative and roughness properties. We also suggest that the water-holding capacity of the soil is the major determinant of the hydrologic thriftiness of the continents, and that it can serve as an excellent surrogate for it.

In the W4 and W60 experiments, two extreme values of hydrologic thriftiness have been employed. It is suggested that most real land surfaces have a hydrologic thriftiness that lies somewhere between those associated with the water-holding capacities of 4 and 60 cm. It is also suggested that the hydrologic thriftiness of most climate models lies within these same bounds. Accepting these suggestions, one could conclude that the large-scale errors in model-computed climates associated with errors in prescriptions of hydrologic thriftiness are bounded by the W60–W4 differences. Given more precise estimates or assumptions of the hydrologic thriftiness of the real world and of a model, the results given here allow a correspondingly more precise statement to be made regarding the errors in that model induced by errors in continental hydrology.

It may also be noted that the physical mechanisms identified in this paper will generally be relevant in determining the sensitivity of a given model climate to its hydrologic parameterization. Thus, in a model whose hydrologic thriftiness is too large, there will be a tendency for excessive evaporation and insufficient runoff. According to the results of the experiments described here, such an error in the tropics will erroneously tend to lower continental surface temperatures, to intensify the Hadley circulation, to weaken monsoonal circulations, and to induce insufficient onshore transport of water vapor. In middle latitudes, excessive hydrologic thriftiness will artificially drop temperatures, raise humidity, and drop vapor flux convergences over land. Insufficient thriftiness in the parameterization will have the opposite effects.

f. Sensitivity of results to model assumptions

Certain parameterizations and other modeling assumptions adopted for this study may distort the sen-

sitivities analyzed in this paper. The most important of these are briefly discussed here.

1) LAND-SURFACE PARAMETERIZATION

The surface parameterization employed in this study is the simplest interactive scheme in use today, and fails to recognize the geographic variability of continental hydrologic response to climate. Because the parameterization tends to ignore limitation of evaporation by surface factors (stomatal resistance, infiltration capacity of soil) other than storage capacity, sensitivities to storage capacity may be overestimated somewhat. Nevertheless, there is no obvious reason to expect that use of a more accurate surface parameterization would alter the basic conclusions of this paper regarding sensitivities and the physical processes that control them.

2) CLOUD RADIATIVE FEEDBACK

It is important to recognize that the sensitivities identified here have been computed using a model with prescribed cloud. We may expect that the noted changes in precipitation would lead to changes in cloud cover, with associated changes in radiation budgets, diabatic heating, circulation, humidity, moisture convergence, temperature and precipitation. A more complete measure of the sensitivity of climate would consist of that identified here plus the cloud feedback.

Preliminary analysis of experiments with interactive clouds supports the conclusions of the present work, and indicates that cloud feedbacks have potentially large impacts on global water and energy cycles. In particular, clouds increase globally as the storage capacity and evaporation increase; their increase causes a net radiative cooling of the atmosphere; the convergence of water vapor flux to the continents is further reduced (relative to the case with prescribed cloud) in the tropics because of circulation changes induced by the changes in radiative heating; and the onshore transient-eddy flux of water vapor in the extratropics increases because of the radiative cooling, hence reduced absolute humidity, of the air over the continents. Major consequences of these feedbacks are that the global surface temperature drops significantly more under interactive cloud than under prescribed cloud; that the increased evaporation associated with the change of storage capacity in the middle and high latitudes is mostly recycled as precipitation onto the continents; and that the precipitation increases in the tropics are realized mostly over the oceans.

3) OCEAN THERMAL FEEDBACK

For computational efficiency and simplicity of analysis, the adjustments of ocean temperatures and sea ice to changes in continental evaporation have not been included in this study; even with a simple mixed-layer model of the ocean, the time scale of adjustment of ocean temperatures is on the order of decades. In our simulations with prescribed ocean surface temperatures, the resulting artificial change in heat flux to the oceans for W60–W4 is 1.3 W m^{-2}, averaged over the ocean area. In contrast, the heat flux to an interactive ocean at equilibrium would vanish. A climate simulation employing an energy-conserving ocean would instead dispose of the extra energy by having a slightly warmer atmosphere, emitting an extra 0.9 W m^{-2} radiation globally to space. In the extreme case that the oceanic atmosphere made the entire radiative adjustment, the diabatic heating contrast between oceanic and continental parts of the atmosphere would be unchanged. In the other extreme where the entire adjustment is made by the continental part of the atmosphere, the W60–W4 change in land/sea diabatic heating contrast would increase from $-6.6/2.8$ W m^{-2} to $-9.7/4.1$ W m^{-2}. (For comparison, the diabatic heating over land/sea for the average of W4 and W60 was $12.2/-5.2$ W m^{-2}, so in any case, the change in heating contrast is quite large.) The sensitivities identified herein that result from land/ocean heating contrasts might therefore have been somewhat larger if ocean thermal feedback had been considered.

Acknowledgments. This paper had the benefit of technical reviews by S. W. Hostetler, B. M. Lofgren, and J. D. Mahlman. Incisive critiques by S. Manabe were especially helpful in defining the scope and structure.

This work was cosponsored by the U.S. Geological Survey and the Geophysical Fluid Dynamics Laboratory of the National Oceanic and Atmospheric Administration.

REFERENCES

Budyko, M. I., 1956: *Heat Balance of the Earth's Surface* Gidrometeoizdat, 255 pp. (in Russian).

——, and A. A. Sokolov, 1978: Water Balance of the Earth. *World Water Balance and Water Resource of the Earth, Studies and Reports in Hydrology,* Vol. 25, V. I. Korzun, Ed., UNESCO Press, 663 pp.

Dickinson, R. E., and A. Henderson-Sellers, 1988: Modelling tropical deforestation: A study of GCM land-surface parameterizations. *Quart J. Roy. Meteor. Soc.,* **114,** 439–462.

Eagleson, P. S., 1978: Climate, soil, and vegetation, 6, Dynamics of the annual water balance. *Water Resour. Res.,* **14,** 749–764.

Gordon, C. T., and W. F. Stern, 1982: A description of the GFDL global spectral model. *Mon. Wea. Rev.,* **110,** 625–644.

Held, I. M., 1983: Stationary and quasi-stationary eddies in the extratropical troposphere: Theory. *Large-Scale Dynamical Processes in the Atmosphere.* B. J. Hoskins and R. P. Pearce, Eds., Academic, 127–168.

Intergovernmental Panel on Climate Change, 1990: *Climate Change.* Cambridge University Press, 365 p.

Lean, J., and D. A. Warrilow, 1989: Simulation of the regional climatic impact of Amazon deforestation. *Nature,* **342,** 411–413.

Manabe, S., 1969: Climate and the ocean circulation, 1. The atmospheric circulation and the hydrology of the earth's surface. *Mon. Wea. Rev.,* **97,** 739–774.

——, J. Smagorinsky, and R. F. Strickler, 1965: Simulated climatology of a general circulation model with a hydrologic cycle. *Mon. Wea. Rev.,* **93,** 769–798.

Milly, P. C. D., 1992: Potential evaporation and soil moisture in general circulation models. *J. Climate,* **5,** 209–226.

——, 1993: An analytic solution of the stochastic storage problem applicable to soil water. *Water Resour. Res.,* **29,** 3755–3758.

Nobre, C. A., P. J. Sellers, and J. Shukla, 1991: Amazonian deforestation and regional climate change. *J. Climate,* **4,** 957–988.

Patterson, K. A., 1990: Global distributions of total and total-available soil water-holding capacities. M.S. thesis, University Delaware, Dept. of Geography, 119 pp. [Available from Morris Library, University of Delaware, Newark, Delaware 19716.]

Penman, H. L., 1948: Natural evaporation from open water, bare soil, and grass. *Proc. Roy. Soc. London,* **A193,** 120–145.

Shiklomanov, I. A., and O. L. Markova, 1987: *Problems of Water Supply and Transfers of River Flow in the World* Gidrometeoizdat, 294 pp. (in Russian).

Shukla, J., and Y. Mintz, 1982: Influence of land-surface evapotranspiration on the earth's climate. *Science,* **215,** 1498–1500.

Shukla, J., C. Nobre, and P. Sellers, 1990: Amazonia deforestation and climate change. *Science,* **247,** 1322–1325.

Vinnikov, K. Ya., P. Ya. Groisman, and K. M. Lugina, 1990: Empirical data on contemporary global climate changes (temperature and precipitation). *J. Climate,* **3,** 662–677.

Yeh, T.-C., R. T. Wetherald, and S. Manabe, 1984: The effect of soil moisture on short-term climate and hydrology change—A numerical experiment. *Mon. Wea. Rev.,* **112,** 474–490.

Zubenok, L. I., 1978: Potential and actual evaporation. *World Water Balance and Water Resources of the Earth, UNESCO Studies and Reports in Hydrology.* Vol. 25. V. I. Korzun, Ed., Unesco Press, 130–139.